ICASSP 2024 - 2024 IEEE International Conference on Acoustics, Speech and Signal Processing (ICASSP) | 979-8-3503-4485-1/24/$31.00 ©2024 IEEE | DOI: 10.1109/ICASSP48485.2024.10446655

NON-UNIFORM FREQUENCY SPACING FOR REGULARIZATION-FREE GRIDLESS DOA

Yifan Wu[1]*, Michael B. Wakin*[2]*, Peter Gerstoft*[1]*, and Yongsung Park*[1]

[1] University of California, San Diego, La Jolla, CA, USA
[2] Colorado School of Mines, Golden, CO, USA

ABSTRACT

Gridless direction-of-arrival (DOA) estimation with multiple frequencies can be applied to acoustic source localization. We formulate this as an atomic norm minimization (ANM) problem and derive a *regularization-free* semi-definite program (SDP) avoiding regularization bias. We also propose a fast SDP program to deal with non-uniform frequency spacing. The DOA is retrieved via irregular Vandermonde decomposition (IVD), and we theoretically guarantee the existence of the IVD. We extend ANM to the multiple measurement vector setting and derive its equivalent regularization-free SDP. *For a uniform linear array* using multiple frequencies, we can resolve more sources than the sensors. The effectiveness of the proposed framework is demonstrated via numerical experiments.

Index Terms— Atomic norm minimization, Multiple frequencies, Vandermonde decomposition, DOA estimation.

1. INTRODUCTION

In the past few decades, some wideband direction-of-arrival (DOA) estimation methods have been proposed [2–7]. Recently proposed methods based on sparse recovery [2–10] and the multi-frequency model [3, 5] have demonstrated superior performance in wideband DOA estimation problems.

The multi-frequency model [2–7] uses N_f (rather than 1) temporal frequency bins in a frequency set $\{F_1, \dots, F_{N_f}\}$ to characterize a wideband signal. All these frequencies are used for DOA estimation, as opposed to using a single frequency under the narrowband model.

Atomic norm minimization (ANM) [11] is a general framework for promoting sparse signal decompositions. The main benefit of ANM is that it overcomes the grid mismatch error that plagues grid-based methods. The pioneering ANM paper [12] proposed an optimization-based continuous (temporal) frequency estimation method and provided a theoretical guarantee when full data are available. The authors in [13] studied continuous temporal frequency estimation based on randomly sampled data for the single measurement vector (SMV) case. ANM for multiple measurement vectors (MMV) under the uniform (or equispaced) time samples was studied [14–16] and was applied to DOA estimation for uniform linear arrays (ULAs) and for non-uniform arrays (NUAs) [17]. It was extended to multiple frequencies for wideband DOA estimation in [5, 18]. The sample complexity of modal analysis with random temporal compression was established in [19]. We refer readers to [20] for an overview of ANM and its applications.

We propose a wideband DOA estimation framework that significantly expands the applicability from [5]. 1) The method in [5] was developed under the SMV case and we extend it to the MMV model. 2) We develop a fast semi-definite program (SDP) for the primal domain SDP. The ANM [5] was formulated as an SDP problem, thus being solved using off-the-shelf SDP solvers, e.g., CVX [21]. The fast SDP is derived based on the dual problem of the fast algorithm [5]. The fast algorithm improves the speed and extends the method to the non-uniform frequency (NUF) case. The DOAs are encoded in a matrix with an *irregular Toeplitz* structure. We apply the irregular Vandermonde decomposition (IVD) [17] to this matrix to retrieve the DOAs. Further, we provide a theoretical guarantee for the existence of the IVD which was not shown in [17]. 3) The developed framework is regularization-free. In [5], regularization was applied to enhance the robustness to noise. However, regularization leads to bias. The proposed framework avoids regularization bias and achieves superior performance. 4) We consider more sources than sensors *under the ULA setup*. For a single frequency, the maximum number of uniquely identifiable sources in an N_M-element ULA is $N_M - 1$ [22, Sec. 11.2.3]. Co-prime array techniques [23] can break this limit with a carefully designed array structure, enabling the resolution of more sources than sensors. We show that *a ULA with multiple frequencies* can resolve more sources than sensors. The physical intuition is that multiple frequencies increase the diversity of the harmonics and these "new harmonics" serve as extra "virtual sensors" in a virtual array.

2. PRELIMINARIES

2.1. Assumptions

The array configuration and signal model are assumed as follows:
1) The array is a ULA with N_M sensors and spacing d.
2) The sources have frequencies drawn from a uniform grid $\{1, \dots, N_F\} \cdot F_1$, where F_1 is the frequency spacing. Let $\lambda_1 := c/F_1$ be the wavelength for F_1, where c is the propagation speed. We assume $\lambda_1 = 2d$ where d is the sensor spacing; equivalently, $d = \frac{c}{2F_1}$. This spacing is for simplifying the derivation and can be relaxed to any $d \leq \frac{\lambda_1}{2}$ (see [5]). We let $\mathcal{F} \subseteq \{1, \dots, N_F\}$ denote the indices of the active source frequencies; the resulting frequencies are thus $\{f \cdot F_1 | f \in \mathcal{F}\}$ with wavelengths $\{\lambda_1/f | f \in \mathcal{F}\}$. We define $N_f := |\mathcal{F}| \leq N_F$ to be the number of active source frequencies. When all frequencies are active, $N_f = N_F$, and we refer to this as the *uniform frequency* case. When only some frequencies are active, $N_f < N_F$, and we refer to this as the *NUF* case.
3) There are N_l snapshots (time samples) received by each sensor. The source amplitude for the f-th frequency ($f \in \mathcal{F}$) is $\mathbf{x}_w(f) = [x_w^{(1)}(f) \ \dots \ x_w^{(N_l)}(f)]^T \in \mathbb{C}^{N_l}$.
4) There are K uncorrelated sources impinging on the array from unknown DOAs θ, or directional cosines $w := F_1 d \cos(\theta)/c = \cos(\theta)/2$.

This work is supported by NSF Grants CCF-1704204, CCF-2203060, and Office of Naval Research (ONR) Grant N00014-21-1-2267. The reader is encouraged to refer to our extended work [1] for details.

2.2. MMV-MF Model

For the multiple measurement vector, multiple frequency (MMV-MF) model, we begin by considering the case of a ULA with uniform frequencies, i.e., $N_f = N_F$ (we incorporate the NUF case in Sec. 4). The received signals can be arranged into a tensor $\mathcal{Y} \in \mathbb{C}^{N_M \times N_l \times N_F}$ (sensors $\times$ snapshots $\times$ frequencies) with the following structure:

$$\mathcal{Y} = \mathcal{X} + \mathcal{N} \tag{1}$$

$$\begin{aligned}\mathcal{X} &= \sum_w c_w [\mathbf{a}(1,w)\mathbf{x}_w^T(1)|...|\mathbf{a}(N_F,w)\mathbf{x}_w^T(N_F)] \\ &= \sum_w c_w \mathbf{A}(w) * \mathbf{X}_w^T\end{aligned} \tag{2}$$

where $\mathbf{a}(f,w) = [1\ e^{-j2\pi wf} \dots e^{-j2\pi wf(N_M-1)}]^T$ $= [1\ \ z^f \dots z^{f(N_M-1)}]^T \in \mathbb{C}^{N_M}$ ($z := e^{-j2\pi w}$) is the array manifold vector for the f-th frequency. $\mathcal{N} \in \mathbb{C}^{N_M \times N_l \times N_F}$ denotes additive Gaussian uncorrelated noise in (1). Denote $\mathbf{A}(w) = [\mathbf{a}(1,w) \dots \mathbf{a}(N_F,w)] \in \mathbb{C}^{N_M \times N_F}$ and $\mathbf{X}_w = [\mathbf{x}_w(1) \dots \mathbf{x}_w(N_F)]^T \in \mathbb{C}^{N_F \times N_l}$. $\mathbf{A}(w) * \mathbf{X}_w^T$ is the "reshaped Khatri-Rao product" defined as $[\mathbf{A}(w) * \mathbf{X}_w^T]_{:f} := \mathbf{a}(f,w)\mathbf{x}_w^T(f)$ $(f = 1, ..., N_F)$. When $N_l = 1$, the above matches the SMV model in [5]. We assume $\|\mathbf{X}_w\|_F = 1$, as the coefficient c_w can used to absorb any other scaling of the source amplitudes via the product $c_w\mathbf{X}_w$.

Finally, we define $N = N_F(N_M-1)+1$, noting that $N_F(N_M-1)$ appears in the largest exponent of any array manifold vector used in the MMV-MF model. Consequently, N will determine the size of certain SDP formulations such as (8).

2.3. Irregular Vandermonde and Toeplitz Matrices

Define some integer-valued vector $\boldsymbol{\gamma} = [\gamma_1 \dots \gamma_{N_\gamma}]^T \in \mathbb{Z}^{N_\gamma}$, complex-valued vector $\mathbf{z} = [z_1 \dots z_{N_z}]^T \in \mathbb{C}^{N_z}$, and $\mathbf{w}(\boldsymbol{\gamma}, z) := [z^{\gamma_1} \dots z^{\gamma_{N_\gamma}}]^T$. For arbitrary dimensions N_γ and N_z, an *irregular Vandermonde matrix* of size $N_\gamma \times N_z$ is a matrix having the form [17, eq. (25)]

$$\mathbf{W} = \mathbf{W}(\boldsymbol{\gamma}, \mathbf{z}) = [\mathbf{z}^{\gamma_1} \dots \mathbf{z}^{\gamma_{N_\gamma}}]^T = [\mathbf{w}(\boldsymbol{\gamma}, z_1) \dots \mathbf{w}(\boldsymbol{\gamma}, z_{N_z})]. \tag{3}$$

Note that when the entries of $\boldsymbol{\gamma}$ form an arithmetic progression, specifically $\boldsymbol{\gamma} = [0 \dots N_\gamma - 1]^T$, $\mathbf{W}(\boldsymbol{\gamma}, \mathbf{z})$ forms a regular Vandermonde matrix.

An (N_γ, N_z)-*irregular Toeplitz matrix* is any matrix $\mathbf{T} \in \mathbb{C}^{N_\gamma \times N_\gamma}$ that can be constructed from an irregular Vandermonde matrix as follows [17, eq. (27)]:

$$\mathbf{T} = \mathbf{W}(\boldsymbol{\gamma}, \mathbf{z})\mathbf{D}\mathbf{W}(\boldsymbol{\gamma}, \mathbf{z})^H, \ \ |\mathbf{z}| = 1, \tag{4}$$

where $\boldsymbol{\gamma} \in \mathbb{Z}^{N_\gamma}$ and $\mathbf{z} \in \mathbb{C}^{N_z}$, and where $\mathbf{D} \in \mathbb{R}^{N_z \times N_z}$ is diagonal. We refer to (4) as an *irregular Vandermonde decomposition (IVD)*. Note that any $N_\gamma \times N_\gamma$ positive semi-definite regular Toeplitz matrix $\mathbf{T}$ with rank N_z has a regular Vandermonde decomposition of the form (4) in which $\boldsymbol{\gamma}$ is an arithmetic progression.

3. ATOMIC NORM MINIMIZATION FOR MMV-MF

In this section, we formulate the atomic norm minimization problem for the MMV-MF model with uniform frequencies. Then, we derive an equivalent SDP that makes the proposed framework computationally feasible.

Define the atomic set

$$\mathcal{A} = \{\mathbf{A}(w) * \mathbf{X}_w^T \mid w \in [-1/2, 1/2], \|\mathbf{X}_w\|_F = 1\}. \tag{5}$$

The atomic norm of a tensor $\mathcal{X} \in \mathbb{C}^{N_M \times N_l \times N_F}$ is defined as $\|\mathcal{X}\|_{\mathcal{A}} := \inf\{\sum_w |c_w| \mid \mathcal{X} = c_w\mathbf{A}(w) * \mathbf{X}_w^T \mid \|\mathbf{X}_w\|_F = 1\}$. The ANM problem for the noise-free case can be expressed as

$$\min_{\mathcal{X}} \quad \|\mathcal{X}\|_{\mathcal{A}} \quad \text{s.t.} \quad \mathcal{Y} = \mathcal{X}. \tag{6}$$

When noise is present, the optimization problem is modified to relax the equality constraint:

$$\min_{\mathcal{X}} \quad \|\mathcal{X}\|_{\mathcal{A}} \quad \text{s.t.} \quad \|\mathcal{Y} - \mathcal{X}\|_{\text{HS}} \le \eta, \tag{7}$$

where $\|\cdot\|_{\text{HS}}$ is the Hilbert-Schmidt norm for the tensor (for a 3D tensor $\|\mathcal{A}\|_{\text{HS}} = \sqrt{\sum_{ijk} |a_{ijk}|^2}$).

Proposition 3.1 *Problem* (6) *is equivalent to the following SDP problem*

$$\begin{aligned}&\max_{\mathcal{Q}, \mathbf{P}_0} \langle \mathcal{Q}, \mathcal{Y} \rangle_{\mathbb{R}} \quad \textit{s.t.} \begin{bmatrix} \mathbf{P}_0 & \widetilde{\mathbf{Q}} \\ \widetilde{\mathbf{Q}}^H & \mathbf{I}_{N_l N_F} \end{bmatrix} \succeq 0, \\ &\sum_{i=1}^{N-k} \mathbf{P}_0(i, i+k) = \delta_k, \widetilde{\mathbf{Q}} = [\mathcal{R}(\mathbf{Q}_1) \dots \mathcal{R}(\mathbf{Q}_{N_F})].\end{aligned} \tag{8}$$

Here, $\mathcal{Q} = [\mathbf{Q}_1| \dots |\mathbf{Q}_{N_F}] \in \mathbb{C}^{N_M \times N_l \times N_F}$ *is the dual variable,* $\mathbf{P}_0 \in \mathbb{C}^{N \times N}$ *is used for DOA extraction,* $\langle \mathcal{Q}, \mathcal{Y} \rangle_{\mathbb{R}} = Re[\sum_{ijk} \mathcal{Q}^*(i,j,k)\mathcal{Y}(i,j,k)]$, $\widetilde{\mathbf{Q}} = [\widetilde{\mathbf{Q}}_1 \dots \widetilde{\mathbf{Q}}_{N_F}] \in \mathbb{C}^{N \times N_l N_F}$, *and* $\widetilde{\mathbf{Q}}_f = \mathcal{R}(\mathbf{Q}_f) : N_M \times N_l \to N \times N_l$ *is a mapping defined as*

$$\mathcal{R}(\mathbf{Q}_f)(i,l) = \begin{cases} \mathbf{Q}_f(m,l) & \textit{for } (i,l) = (f(m-1)+1, l) \\ 0 & \textit{otherwise}. \end{cases} \tag{9}$$

Across all frequencies, $\mathcal{R} : N_M \times N_l \times N_F \to N \times N_l N_F$ is a linear mapping and can be expressed as a tall binary matrix multiply $\text{vec}(\widetilde{\mathbf{Q}}) = \mathbf{R}\,\text{vec}(\mathcal{Q})$. $\mathbf{R}^T$ describes the behavior of the adjoint operator $\mathcal{R}^* : N \times N_l N_F \to N_M \times N_l \times N_F$.

In the noisy case, the equivalent SDP of (7) is the regularized version of (8), η depends on the noise level and is the same as in (7):

$$\begin{aligned}&\max_{\mathcal{Q}, \mathbf{P}_0} \langle \mathcal{Q}, \mathcal{Y} \rangle_{\mathbb{R}} - \eta\|\mathcal{Q}\|_{\text{HS}} \quad \text{s.t.} \begin{bmatrix} \mathbf{P}_0 & \widetilde{\mathbf{Q}} \\ \widetilde{\mathbf{Q}}^H & \mathbf{I}_{N_l N_F} \end{bmatrix} \succeq 0, \\ &\sum_{i=1}^{N-k} \mathbf{P}_0(i, i+k) = \delta_k, \widetilde{\mathbf{Q}} = [\mathcal{R}(\mathbf{Q}_1) \dots \mathcal{R}(\mathbf{Q}_{N_F})].\end{aligned} \tag{10}$$

4. REGULARIZATION-FREE FAST ALGORITHM

In this section, we derive a reduced-dimension version of the SDP that can be applied to non-uniform frequency settings. The so-called fast program improves the speed, and more importantly, it relaxes the uniform frequency assumption.

4.1. Non-uniform Frequency (NUF) Setting

In Sec. 3, we focused on the uniform frequency case. We generalize the proposed framework to the NUF case in this section. Recall that $\mathcal{F} \subseteq \{1, \dots, N_F\}$ denotes the indices of the active source frequencies, with $N_f := |\mathcal{F}| \le N_F$ denoting the number of active frequencies. The NUF case corresponds to the scenario where $N_f < N_F$, i.e., only some of the frequencies are active.

Recall that every exponent in an array manifold vector from the MMV-MF model involves a product of one temporal frequency and

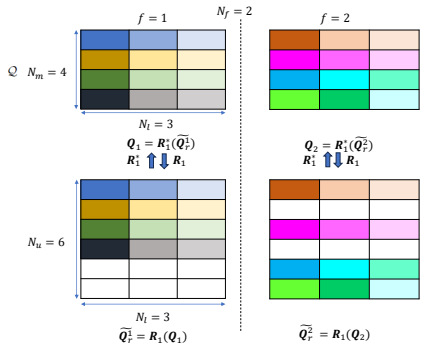

Fig. 1. Demonstration for the $\mathcal{R}_1(\cdot)$ mapping and its adjoint mapping $\mathcal{R}_1^*(\cdot)$. $N_M = 4$, $N_l = 3$, $N_f = N_F = 2$, $\mathcal{U} = \{0,1,2,3,4,6\}$, $N_u = |\mathcal{U}| = 6$.

one sensor position. To capture all such products in the NUF setting, we define a spatial-frequency index set $\mathcal{U}$ as $\mathcal{U} = \{m \cdot f | m \in \mathcal{M}, f \in \mathcal{F}\}$, where $\mathcal{M} = \{0,1,\ldots,N_M-1\}$ denotes the indices of the sensor positions in the ULA. The cardinality of this set $N_u := |\mathcal{U}| \le N = N_F(N_M-1)+1$. In many settings, $N_u \ll N$. In later sections, we see that the size of the fast SDP depends on N_u, and its complexity is greatly reduced compared to the original SDP.

4.2. Fast Dual SDP for the NUF Case

We now generalize the SDP in Proposition 3.1 to the NUF case. Inspired by the fast algorithm in [5, Sec. III-F], the SDP in this section is considered the fast algorithm for MMV.

For NUF, the measurement tensor $\mathcal{Y} \in \mathbb{C}^{N_M \times N_l \times N_f}$ and the SDP in Proposition 3.1 is generalized as

$$\begin{aligned} &\max_{\mathcal{Q},\mathbf{P}_{r0}} \langle \mathcal{Q}, \mathcal{Y} \rangle_{\mathbb{R}} \quad \text{s.t.} \begin{bmatrix} \mathbf{P}_{r0} & \widetilde{\mathbf{Q}}_r \\ \widetilde{\mathbf{Q}}_r^H & \mathbf{I}_{N_l N_f} \end{bmatrix} \succeq 0, \\ &\sum_{\mathcal{U}_j - \mathcal{U}_i = k} \mathbf{P}_{r0}(i,j) = \delta_k, \widetilde{\mathbf{Q}}_r = [\mathcal{R}_1(\mathbf{Q}_1) \ldots \mathcal{R}_1(\mathbf{Q}_{N_f})], \end{aligned} \tag{11}$$

where $\mathcal{Q} = [\mathbf{Q}_1 | \ldots | \mathbf{Q}_{N_f}] \in \mathbb{C}^{N_M \times N_l \times N_f}$ is the dual variable, $\mathbf{P}_{r0} \in \mathbb{C}^{N_u \times N_u}$, $\widetilde{\mathbf{Q}}_r = [\widetilde{\mathbf{Q}}_r^1 \ldots \widetilde{\mathbf{Q}}_r^{N_f}] \in \mathbb{C}^{N_u \times N_l N_f}$ ($\widetilde{\mathbf{Q}}_r^f = \mathcal{R}_1(\mathbf{Q}_f) \in \mathbb{C}^{N_u \times N_l}$), and $\mathcal{R}_1(\mathbf{Q}_f) : N_M \times N_l \to N_u \times N_l$ is a mapping that pads zeros to the extra entries defined as

$$\mathcal{R}_1(\mathbf{Q}_f)(r,l) = \begin{cases} \mathbf{Q}_f(m,l) & \text{for } (\mathcal{U}_r, l) = (f \cdot (m-1), l) \\ 0 & \text{otherwise.} \end{cases} \tag{12}$$

Fig. 1 demonstrates the $\mathcal{R}_1(\cdot)$ mapping. Any rows of $\widetilde{\mathbf{Q}}_f$ which would have remained all-zero under the operator $\mathcal{R}(\cdot)$ (corresponding to unused space-frequency products) are omitted in $\mathcal{R}_1(\cdot)$.

Comparing (12) with (9), these two mappings pad zeros for the same input $\mathbf{Q}_f$ to obtain the output matrix with a different dimension. As a result, (11) not only gives a lower-dimensional formulation (the size of $\mathbf{P}_{r0}$ decreases from $N \times N$ to $N_u \times N_u$), but it naturally accommodates the NUF setting. Still, (11) can be applied to the uniform frequency case, where N_u is often smaller than N.

4.3. Fast Primal SDP for the NUF Case

We now derive the dual problem of (11), yielding a fast primal SDP that is regularization-free and accommodates the NUF setting.

Proposition 4.1 *The dual problem of* (11) *is given by*

$$\begin{aligned} &\min_{\mathbf{W},\mathbf{u},\widetilde{\mathbf{Y}}} [\mathrm{Tr}(\mathrm{T}(\mathbf{u})) + \mathrm{Tr}(\mathbf{W})] \\ &\text{s.t.} \begin{bmatrix} \mathrm{T}(\mathbf{u}) & \widetilde{\mathbf{Y}} \\ \widetilde{\mathbf{Y}}^H & \mathbf{W} \end{bmatrix} \succeq 0, \mathbf{Y}_f = \mathcal{R}_1^*(\widetilde{\mathbf{Y}}_f), f \in \mathcal{F}, \end{aligned} \tag{13}$$

where $\widetilde{\mathbf{Y}} \in \mathbb{C}^{N_u \times N_l N_f}$, $\mathbf{W} \in \mathbb{C}^{N_l N_f \times N_l N_f}$, $\mathbf{Y}_f \in \mathbb{C}^{N_M \times N_l}$ *is the slice of the received signal tensor* $\mathcal{Y}$ *corresponding to frequency* f, *and* $\widetilde{\mathbf{Y}}_f \in \mathbb{C}^{N_u \times N_l}$ *comes from taking the* N_l *columns of* $\widetilde{\mathbf{Y}}$ *corresponding to frequency* f. $\mathcal{R}_1^*(\cdot) : N_u \times N_l \to N_M \times N_l$ *is the adjoint mapping of* $\mathcal{R}_1$. $\mathbf{u} \in \mathbb{C}^{N \times 1}$, *and* $\mathrm{T} : N \times 1 \to N_u \times N_u$ *is explicitly defined as (note* * *denotes complex conjugate)*

$$\mathrm{T}(\mathbf{v})(i,j) := \begin{cases} v_{\mathcal{U}_j - \mathcal{U}_i} & \mathcal{U}_j - \mathcal{U}_i \ge 0 \\ v_{\mathcal{U}_i - \mathcal{U}_j}^* & \mathcal{U}_j - \mathcal{U}_i < 0. \end{cases}$$

Remark The dual problem of (8) can be similarly derived, yielding the following full-dimension primal SDP for the ULA and uniform frequency case:

$$\begin{aligned} &\min_{\mathbf{W},\mathbf{u},\widetilde{\mathbf{Y}}_N} [\mathrm{Tr}(\mathrm{Toep}(\mathbf{u})) + \mathrm{Tr}(\mathbf{W})] \\ &\text{s.t.} \begin{bmatrix} \mathrm{Toep}(\mathbf{u}) & \widetilde{\mathbf{Y}}_N \\ \widetilde{\mathbf{Y}}_N^H & \mathbf{W} \end{bmatrix} \succeq 0, \mathbf{Y}_f = \mathcal{R}^*(\widetilde{\mathbf{Y}}_{Nf}), f = 1,\ldots,N_F, \end{aligned} \tag{14}$$

where $\mathrm{Toep}(\cdot) : N \times 1 \to N \times N$ is the Toeplitz operator that maps a vector to a self-adjoint Toeplitz matrix. $\widetilde{\mathbf{Y}}_N \in \mathbb{C}^{N \times N_l N_F}$, $\mathcal{R}^*(\cdot) : N \times N_l \to N_M \times N_l$ is the adjoint mapping of $\mathcal{R}(\cdot)$, and $\widetilde{\mathbf{Y}}_{Nf} \in \mathbb{C}^{N \times N_l}$ is taking N_l columns from $\widetilde{\mathbf{Y}}_N$ (from the $(f-1)\cdot N_l+1$-th to the $f \cdot N_l$-th column). Compared to (13), a main difference is that $\mathrm{T}(\mathbf{u}) \in \mathbb{C}^{N_u \times N_u}$ in (13) is changed to $\mathrm{Toep}(\mathbf{u}) \in \mathbb{C}^{N \times N}$.

4.4. Existence of Irregular Vandermonde Decomposition (IVD)

In ANM problems that involve trace minimization of a regular Toeplitz matrix, one typically computes the Vandermonde decomposition of the resulting Toeplitz matrix to extract the DOAs.

In contrast, the fast primal SDPs (13) derived in the previous section involve trace minimization not of a Toeplitz matrix but rather a matrix of the form $\mathrm{T}(\mathbf{u})$. However, as we establish in Theorem 4.2 below, there is an important connection between $\mathrm{T}(\mathbf{u})$ and Toeplitz matrices: $\mathrm{T}(\mathbf{u})$ is guaranteed to be an irregular Toeplitz matrix, and therefore is guaranteed to have an IVD.

Theorem 4.2 *For any* $\mathbf{u}$ *such that* $\mathrm{Toep}(\mathbf{u})$ *is PSD,* $\mathrm{T}(\mathbf{u}) \in \mathbb{C}^{N_u \times N_u}$ *is an* (N_u, K)*-irregular Toeplitz matrix, where* $K = \mathrm{rank}(\mathrm{Toep}(\mathbf{u}))$. *Specifically,* $\mathrm{T}(\mathbf{u})$ *has an IVD of the form* (4), *where* $\boldsymbol{\gamma} = [\mathcal{U}_1, \ldots \mathcal{U}_{N_u}]^T$.

In summary, we first solve the SDP (13) via an SDP solver (e.g., CVX [21]). After $\mathbf{u}$ is obtained, the DOAs are retrieved by IVD methods (e.g., root-MUSIC). Although (13) is regularization-free, it is robust to noise and the robustness is achieved by IVD.

5. MORE SOURCES THAN SENSORS IN THE ULA SETUP

For single-frequency ULA, the maximum number of resolvable sources is $N_M - 1$ [22, Sec 11.2.3]. In this section, we will demonstrate the possibility of resolving more sources than sensors *under the ULA setup* if multiple frequencies are available. In our multi-frequency ANM configuration, it can resolve up to

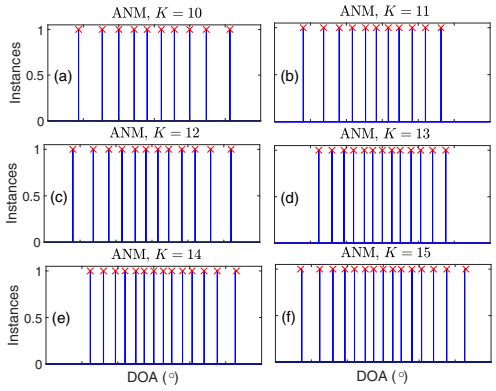

Fig. 2. Estimated and True DOAs for ANM ("×" indicates the true DOAs and the blue vertical line indicates the estimated DOAs). $N_M = 4$, $N_F = 5$, $N_l = 1$, and $K = 10, 11, 12, 13, 14, 15$. The RMSEs of ANM under $K = 10, 11, 12, 13, 14, 15$ are $0.005°$, $0.16°$, $0.20°$, $0.04°$, $0.27°$, and $0.27°$.

$N - 1 = (N_M - 1)N_F$ sources as $\text{Toep}(\mathbf{u}) \in \mathbb{C}^{N\times N}$ and $\mathbf{U}_N$ exists only if $K \leq N - 1$. The reason for using (14) instead of (13) is that (13) can resolve up to $N_u - 1$ sources and (14) has the potential to resolve more sources than (13) because $\text{Toep}(\mathbf{u})$ in (14) has a higher dimension than $\text{T}(\mathbf{u})$ in (13).

The key observation for the multi-frequency model is that these frequencies increase the diversity of the harmonics. These extra harmonics serve as "virtual" sensors in the array, and they bring about an enhanced degree of freedom. The SDP problem (13) can be interpreted as a structured covariance matrix estimation problem ($\text{T}(\mathbf{u})$ can be interpreted as the covariance matrix). We notice this covariance matrix is in a higher dimension, which corresponds to our intuition that there are more sensors in our "virtual" array.

As an example, suppose we have $N_M = 4$ sensors, $N_F = 5$ frequencies ($\{100, \ldots, 500\}$ Hz), $N_l = 1$ snapshot, noise-free, and $K = 10, 11, 12, 13, 14, 15$ sources with uniform and deterministic across frequencies. For $K = 10, 12$, and 15, the DOAs are generated as the uniform distribution in the cosine domain (i.e., the DOAs are $\lfloor \cos^{-1}(-1 + 2([1:K] - 0.5)/K) \rfloor$). For $K = 11$, we pick up the last 11 sources in the $K = 12$ case. For $K = 13$, we pick up the middle 13 sources in the $K = 15$ case, and for $K = 14$, we pick up the middle 14 sources. We plot the estimated DOAs for ANM. From Fig. 2, our ANM can resolve up to $(N_M - 1)N_F = 15$ sources.

6. SIMULATION RESULTS

The simulation setup is detailed as follows. The source amplitude is complex Gaussian. N_l snapshots are collected. The uniform frequency set is defined as $\{1, \ldots, N_F\} \cdot F_1$ (F_1 is the minimum frequency). The array spacing for ULA is $\frac{\lambda_1}{2}$ where λ_1 is the wavelength for the minimum frequency in the frequency set. The noise for each frequency and each snapshot is randomly generated from the complex Gaussian distribution $\mathcal{CN}(0, \sigma^2)$ and then scaled to fit the desired signal-to-noise ratio (SNR): $\text{SNR} = 20\log_{10} \|\mathcal{X}\|_{\text{HS}} / \|\mathcal{N}\|_{\text{HS}}$.

In the Monte-Carlo experiments, $MC = 100$ trials are executed to compute the root mean square error (RMSE) defined as

$$\text{RMSE} = \sqrt{\frac{1}{MC}\sum_{m=1}^{MC}\left[\min\left(\frac{1}{K}\sum_{k=1}^{K}(\hat{\theta}_{mk} - \theta_{mk})^2, 10^2\right)\right]},$$

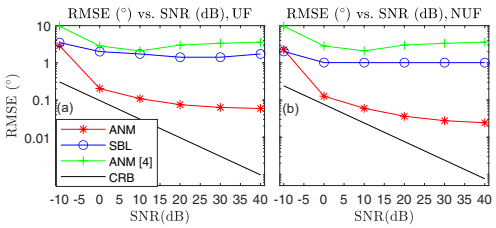

Fig. 3. RMSE (°) vs. SNR. $N_M = 16$ ULA with $d = \lambda_{100}/2$. $N_l = 1$. (a) $N_F = 4$ with uniform frequencies $\{100, 200, 300, 400\}$ Hz; (b) $N_F = 4$ with non-uniform frequencies $\{100, 200, 300, 500\}$ Hz. "ANM" and "ANM [4]" represents the proposed framework and the framework proposed in [5].

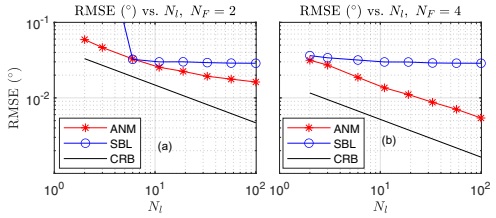

Fig. 4. RMSE (°) vs. N_l for MMV setup. $N_M = 16$ ULA with $d = \lambda_{100}/2$. $K = 3$ DOAs at $[88°, 93°, 155°] + \boldsymbol{\epsilon}$ where $\boldsymbol{\epsilon}$ contains random offsets from a uniform distribution $[0, 1]$. SNR = 20 dB. (a): $N_F = 2$ with frequency set $\{100, 200\}$ Hz; (b) $N_F = 4$ with frequency set $\{100, 200, 300, 400\}$ Hz.

where $\hat{\theta}_{mk}$, and θ_{mk} are (sorted) estimated DOAs, and (sorted) ground-truth DOAs for the kth DOA and mth trial. A maximum threshold of $10°$ is used to penalize the incorrect DOA estimates. We compare the proposed method with the multi-frequency sparse Bayesian learning (SBL) [3]. The Cramér-Rao bound (CRB) [24, Eq. (121)] for the multi-frequency model is computed for reference.

We examine the performance under the non-uniform frequency set. In this case, $N_f = 4$, and the frequency set is $\{100, 200, 300, 500\}$ Hz. Fig. 3(b) demonstrates the effectiveness of the proposed method under the non-uniform frequency case. We also see superior performance compared to the fast dual algorithm in [5] in both uniform and non-uniform frequency cases.

We then examine the performance of ANM with varying numbers of snapshots N_l. From Fig. 4, we can see ANM follows the trend of CRB and outperforms SBL. We also see that more snapshots will improve the performance. In addition, comparing Fig. 4(a) with 4(b), ANM performs better with higher N_F, which demonstrates the benefits of multi-frequency processing.

7. CONCLUSION

This paper proposes a gridless DOA estimation method based on *regularization-free* SDP and Vandermonde decomposition. We extend this framework to MMV and NUF cases. For the NUF case, the Toeplitz structure will not hold. However, we propose to use IVD in these cases, and the existence of IVD is theoretically guaranteed. With the help of multiple frequencies, the method can resolve more sources than the number of physical sensors under the ULA setup. Simulations demonstrate the proposed framework can achieve superior performance for MMV and NUF setups.

8. REFERENCES

[1] Y. Wu, M. B. Wakin, and P. Gerstoft, "Non-uniform array and frequency spacing for regularization-free gridless DOA," *arXiv preprint arXiv:2401.06313*, 2024.

[2] N. Antonello, E. De Sena, Marc Moonen, P. A. Naylor, and T. van Waterschoot, "Joint acoustic localization and dereverberation through plane wave decomposition and sparse regularization," *IEEE/ACM Trans. Audio, Speech, Lang. Process.*, vol. 27, no. 12, pp. 1893–1905, 2019.

[3] S. Nannuru, K. L. Gemba, P. Gerstoft, W. S. Hodgkiss, and C. F. Mecklenbräuker, "Sparse Bayesian learning with multiple dictionaries," *Signal Process.*, vol. 159, pp. 159–170, 2019.

[4] K. L. Gemba, S. Nannuru, and P. Gerstoft, "Robust ocean acoustic localization with sparse Bayesian learning," *IEEE J. Sel. Topics Signal Process.*, vol. 13, no. 1, pp. 49–60, 2019.

[5] Y. Wu, M. B. Wakin, and P. Gerstoft, "Gridless DOA estimation with multiple frequencies," *IEEE Trans. Signal Process.*, vol. 71, pp. 417–432, 2023.

[6] Z. Tang, G. Blacquiere, and G. Leus, "Aliasing-free wideband beamforming using sparse signal representation," *IEEE Trans. Signal Process.*, vol. 59, no. 7, pp. 3464–3469, 2011.

[7] K. L. Gemba, S. Nannuru, P. Gerstoft, and W. S. Hodgkiss, "Multi-frequency sparse Bayesian learning for robust matched field processing," *J. Acoust. Soc. Am.*, vol. 141, no. 5, pp. 3411–3420, 2017.

[8] J. Zhang, N. Hu, M. Bao, X. Li, and W. He, "Wideband DOA estimation based on block FOCUSS with limited samples," in *IEEE GlobalSIP*, 2013, pp. 634–637.

[9] L. Wang, L. Zhao, G. Bi, C. Wan, L. Zhang, and H. Zhang, "Novel wideband DOA estimation based on sparse Bayesian learning with Dirichlet process priors," *IEEE Trans. Signal Process.*, vol. 64, no. 2, pp. 275–289, 2015.

[10] C. Liu, Y. V. Zakharov, and T. Chen, "Broadband underwater localization of multiple sources using basis pursuit denoising," *IEEE Trans. Signal Process.*, vol. 60, no. 4, pp. 1708–1717, 2011.

[11] V. Chandrasekaran, B. Recht, P. A. Parrilo, and A. S. Willsky, "The convex geometry of linear inverse problems," *Found. Comput. Math.*, vol. 12, no. 6, pp. 805–849, 2012.

[12] E. J. Candès and C. Fernandez-Granda, "Towards a mathematical theory of super-resolution," *Commun. Pure Appl. Math.*, vol. 67, no. 6, pp. 906–956, 2014.

[13] G. Tang, B. N. Bhaskar, P. Shah, and B. Recht, "Compressed sensing off the grid," *IEEE Trans. Inf. Theory*, vol. 59, no. 11, pp. 7465–7490, 2013.

[14] Y. Li and Y. Chi, "Off-the-grid line spectrum denoising and estimation with multiple measurement vectors," *IEEE Trans. Signal Process.*, vol. 64, no. 5, pp. 1257–1269, 2015.

[15] Z. Yang and L. Xie, "Exact joint sparse frequency recovery via optimization methods," *IEEE Trans. Signal Process.*, vol. 64, no. 19, pp. 5145–5157, 2016.

[16] Z. Yang, J. Tang, Y. C. Eldar, and L. Xie, "On the sample complexity of multichannel frequency estimation via convex optimization," *IEEE Trans. Inf. Theory*, vol. 65, no. 4, pp. 2302–2315, 2018.

[17] M. Wagner, Y. Park, and P. Gerstoft, "Gridless DOA estimation and root-MUSIC for non-uniform linear arrays," *IEEE Trans. Signal Process.*, vol. 69, pp. 2144–2157, 2021.

[18] Y. Wu, M. B. Wakin, and P. Gerstoft, "Gridless DOA estimation under the multi-frequency model," in *IEEE ICASSP*, 2022, pp. 5982–5986.

[19] S. Li, D. Yang, G. Tang, and M. B. Wakin, "Atomic norm minimization for modal analysis from random and compressed samples," *IEEE Trans. Signal Process.*, vol. 66, no. 7, pp. 1817–1831, 2018.

[20] Y. Chi and M. F. Da Costa, "Harnessing sparsity over the continuum: Atomic norm minimization for superresolution," *IEEE Signal Process. Mag.*, vol. 37, no. 2, pp. 39–57, 2020.

[21] M. Grant and S. Boyd, "CVX: Matlab software for disciplined convex programming, version 2.1," 2014.

[22] Z. Yang, J. Li, P. Stoica, and L. Xie, "Sparse methods for direction-of-arrival estimation," in *Academic Press Library in Signal Processing, Volume 7*, pp. 509–581. Elsevier, 2018.

[23] P. P. Vaidyanathan and P. Pal, "Sparse sensing with co-prime samplers and arrays," *IEEE Trans. Signal Process.*, vol. 59, no. 2, pp. 573–586, 2010.

[24] Y. Liang, W. Liu, Q. Shen, W. Cui, and S. Wu, "A review of closed-form Cramér-Rao bounds for DOA estimation in the presence of gaussian noise under a unified framework," *IEEE Access*, vol. 8, pp. 175101–175124, 2020.